Received: 20 February 2024 | Revised: 6 May 2024 | Accepted: 8 May 2024

DOI: 10.1002/dep2.289

ORIGINAL RESEARCH ARTICLE

The Depositional Record Open Access
A journal of the International Association of Sedimentologists
IAS WILEY

Evolution of a late Quaternary succession by interpretation of high-resolution seismic and bathymetric data, Adriatic Sea

Federico Da Col | **Massimo Zecchin** | **Dario Civile** | **Luca Baradello** | **Michele Deponte** | **Flavio Accaino**

Istituto Nazionale di Oceanografia e di Geofisica Sperimentale—OGS, Trieste, Italy

Correspondence
Federico Da Col, Istituto Nazionale di Oceanografia e di Geofisica Sperimentale—OGS, Trieste, Italy.
Email: fdacol@ogs.it

Funding information
European Commission; Interreg

Abstract

This paper presents the results of the interpretation of a set of high-resolution seismic lines integrated with multibeam echosounder data acquired in a coastal area in the Northern Adriatic Sea. The aim of the study was to reconstruct the stratigraphic evolution of a late Quaternary sedimentary succession offshore the town of Bibione, North-Eastern Italy, by recognising the key unconformities, identifying the main depositional units, dating them and reconstructing the depositional environments in relation to relative sea-level variations. Specifically, four sedimentary units, separated by erosional unconformities associated with the development of deep channels, were identified and dated based on literature information. By interpreting the seismic data, sedimentary dynamics were reconstructed and palaeoenvironments identified. The lower unit corresponds to a paludal environment, showing abundant gas seeps and accumulations (bright spots); the two intermediate units correspond to fluvial deposits, filling the deep incisions that characterise the bounding surfaces. Finally, the shallowest unit, bounded by a wave-ravinement surface incised by tidal currents, corresponds to the Holocenic progradation of the coastal wedge. In addition, several vertical gas chimneys were identified, ranging in width from a few metres to 20–30 m. These were present in all units, often reaching the sea floor. Finally, elongated mounds, about 300 m wide, at the sea floor were recognised. The bathymetric and seismic characteristics of these elongated bodies and their relationship to adjacent sedimentary bodies suggest that they are probably methane-derived carbonate formations known as 'Trezze' or 'Tegnùe'. These names recall the fact that the trawls of the local fishermen were often hindered ('tegnù' in the Venetian language) or even cut off by these formations.

KEYWORDS

Adriatic Sea, high-resolution seismic, Last Glacial Maximum, multibeam echosounding, Quaternary Geology

1 | INTRODUCTION

The coasts of the northern Adriatic are characterised by the presence of marshlands and the much studied lagoons (Fontolan et al., 2007; Bondesan & Meneghel, 2004). These coastal sedimentary systems have evolved as the result of the balance between the sediments transported by the rivers and tidal inlets and the erosion caused by the sea. Furthermore, both the plain and the sea floor show a very low gradient (*ca* 0.4‰, Ronchi et al., 2018). Due to the cultural, historical and economic importance of the Venice lagoon and the Veneto-Friuli plain (North-Eastern Italy; see Figure 1 for the location), numerous studies have been carried out to reconstruct the geological evolution of the area. The northern Adriatic represents an excellent case to study the impact of a fast relative sea-level rise, both on the environment and on pre-historic human communities (Fontana, 2006; Fontana et al., 2008). Given the current perspectives of a warming global mean temperature, understanding the effects of sea-level rise on a low-gradient plain is of interest for other areas showing similar features.

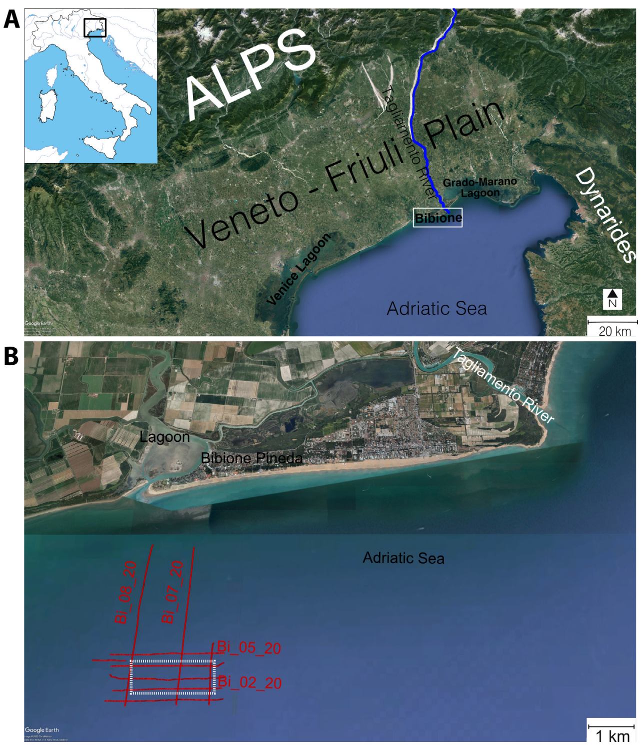

FIGURE 1 (A) Regional context of North-Eastern Italy. The features outlined in the Geological Context section are indicated. The white rectangle indicates the area shown in (B). The figure was generated with Google Earth Pro on 9 April 2024. (B) Georeferenced map of the survey lines: the red lines indicate the location of the Boomer lines, while the white dashed rectangle indicates the location of the multibeam survey. The figure was generated with Google Earth Pro on 9 April 2024.

The oldest studies regarding this area mainly focussed on the post-Last Glacial Maximum (LGM) sedimentation (Gatto & Previatello 1974; Bortolami et al., 1977; Favero & Serandrei Barbero 1980), whereas more recent studies reconstructed the stratigraphic evolution, commencing from an episode of aggradation that occurred during the Tyrrhenian period (Fontana et al., 2010b; Ghielmi et al., 2010; Ronchi et al., 2018). As in most other cases, the evolution of the continental shelf in this area is mainly influenced by Quaternary sea-level changes, so that the geomorphology of the area is the result of multiple glacial–interglacial cycles (Blum & Törnqvist, 2000; Breda et al., 2016). The main event that has been responsible for shaping the study area is the LGM, *ca* 20 ka BP, and the consequent sea-level drop and lowstand phase (Ronchi et al., 2021). During the LGM and the transition from the LGM to the Holocene, deep fluvial incisions developed in the study area (Ronchi et al., 2021). The importance of incised valleys, as they occur in the study area, has been investigated in several studies (Thomas & Anderson, 1989; Blum & Tornqvist, 2000; Blum et al., 2013; Ronchi et al., 2021). In fact, these incised valleys and their sedimentary infills can provide important information regarding the environmental context of the past, covering a long period of time. Specifically, their late Quaternary fills are often the only available source of information on the lowstand and transgressive phases of the continental shelf (Blum et al., 2013; Clement & Fuller, 2018; Ronchi et al., 2018, 2021).

This paper characterises the late Quaternary sedimentary evolution of the succession offshore the coastal town of Bibione, Metropolitan City of Venice, Italy. The aim is to identify the sedimentary units and bounding surfaces, date them and reconstruct the depositional environments in relation to the available literature regarding adjacent areas. A plausible interpretation is proposed for some elongated bodies observed on the sea floor. To achieve this, high-resolution seismic data together with multibeam morpho-bathymetric data were acquired, processed and interpreted. The Bibione area has already been investigated in the past (Bondesan & Meneghel, 2004; Francese et al., 2014; Accaino et al., 2023), but these studies mostly focus on data acquired onshore. The offshore sectors have not been the subject of detailed prior study; this paper addresses this knowledge gap.

2 | GEOLOGICAL SETTING

The investigated area is located 1.5 km offshore the town of Bibione Pineda (see Figure 1), 5 km west of the estuary of the Tagliamento River, and the study area covers an area of 3 km in a longitudinal direction and 3.5 km in a latitudinal direction. The Tagliamento River has an average annual discharge rate of 90 m^3/s. However, the river catchment is subject to very high precipitation rates, among the highest in Europe (Borga et al., 2005), and it is also prone to extreme rainfall events that cause floods (Dallan et al., 2022). The maximum discharge rate with a recurrence time of 100 years reaches 4500 m^3/s (Surian & Fontana, 2017). Geologically, the study area represents the offshore part of the Veneto-Friuli alluvial plain (Fontana et al., 2010a), which is bounded to the north by the south-verging chain of the eastern Southern Alps and to the east by the NW-trending thrust belt of the Dinarides (Ghielmi et al., 2010; Ronchi et al., 2021). The main active faults are located along the mountain front and have caused major earthquakes (for a map of the main faults in the area, see figure 1 in Slejko et al., 1999; a more detailed assessment on the faults closest to the study area can be found in Anselmi et al., 2011). The plain occupies the upper part of the foredeep basin of the two chains and is subject to considerable subsidence; Antonioli et al. (2009) estimate an average of 0.4 mm/a, which can, however, reach 10 mm/a locally.

Of particular relevance to this study, the area lies in the Tagliamento megafan, which formed during the aggradational period corresponding to the LGM (29–19 ka BP; Ronchi et al., 2021). The sea-level falls to a low point at or about the time the LGM resulted in a regression of the coastline approximately 300 km to the south from its present-day position, along the Pescara–Sebenico/Šibenik line, at the margins of the Meso-Adriatic depression (Pellegrini et al., 2017; Fontana & Ronchi, 2019). Fontana et al. (2008) reconstructed the areal extent of the megafan to occupy 1200 km^2. The megafan is characterised by an apical part, formed by coarser grained, relatively more permeable sediments, and a distal part, formed by finer grained, relatively less permeable sediments. At the boundary between the two, groundwater is forced to the surface, forming several minor rivers. These rivers, together with the branches of the Tagliamento, were responsible for the incision of the distal part of the megafan during the lowstand, which reached its climax during the LGM. During this same period, aggradation occurred by filling of the fluvial incisions, passing laterally to floodplain deposits. The regression of the coastline started at 19,600 ka BP and was a non-linear process, guided mostly by global climate and to a lesser extent by the retreat of the Alpine glaciers (Antonioli et al., 2009). Given the very low gradient of the distal part of the megafan (*ca* 0.4‰, Ronchi et al., 2018), the marine transgression occurred rapidly. Three major steps in sea-level rise have been recognised: (i) 19.6 ka BP, (ii) 14.6 to 13 ka BP, when a rise of 25 m in 1500 years occurred (Fontana & Ronchi, 2019) and (iii) 11.7 ka BP (Asioli et al., 2001; Fontana et al., 2019). After this last step, at about 7.5 ka BP, the rate of sea-level rise slowed significantly and the position of the current coastline was reached 7.5–5 ka BP, leading to the submersion of the study area (Amorosi et al., 2008; Fontana & Ronchi, 2019). At the survey location, fluvial aggradation therefore continued until that time. During the regression of the coastline, large lagoons, similar both in size and environment to those that can be seen today, were formed and the fluvial channels served as estuaries of the rivers, or as tidal channels and inlets.

3 | METHODS

The marine seismic data were acquired using a Boomer system. This consists of an acoustic source made of an electro-dynamic transducer mounted on a catamaran frame, producing a theoretical minimum-phase wavelet with an amplitude spectrum between 400 and 4000 Hz. This source, suspended at a constant depth of 40 cm, produces a short impulse of energy every 0.5 s. The receiver consists of an array of hydrophones, the traces of which are stacked to reduce random noise. The streamer was kept as shallow as possible to avoid destructive interference between reflected signals and multiple events from the air/water interface (ghost).

The boat towing the acquisition was travelling at a speed of 3 or 4 knots, so that the distance between traces was 0.8–1 m. In order to minimise the noise and the spatial filtering produced by the hydrophones array, the streamer was towed near the source with a 15 m longitudinal offset and a 3.5 m lateral offset (Baradello & Carcione, 2008).

The presence of only long-wavelength, low-amplitude sea waves ensured high-quality data and no tidal correction was necessary. Four lines which were considered to be the most significant are shown in Figures 2 and 3, the positions of which are indicated in Figure 1B.

In the same area where the boomer data were acquired, a survey using a multibeam echosounder was performed. The position of the survey is indicated by the white dashed line in Figure 1B; the resulting image is shown in Figure 4. The multibeam data have enabled a full coverage bathymetric map with a pixel size of 10 cm to be generated. This is achieved using 512 simultaneous beams, equidistant on the sea floor with a swath wide angle of 120–165°. The along-track resolution is directly determined by the speed of the vessel and the ping rate of the sounder, whereas the across-track resolution is determined by the nadir-depth and the angle of the swath. Both these resolutions are

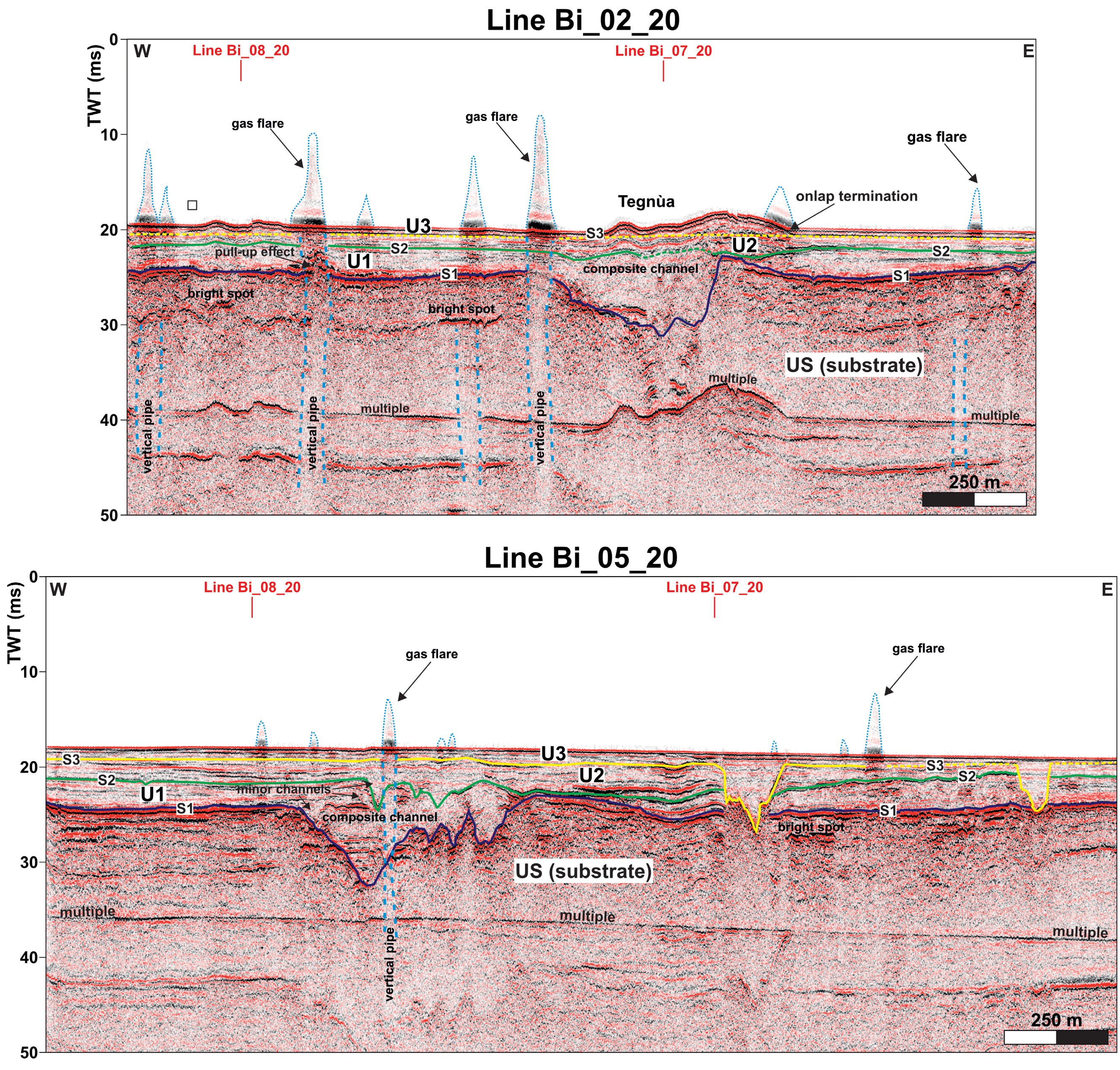

FIGURE 2 Interpreted seismic sections of the boomer data acquired in a latitudinal direction. The location of each line is indicated in Figure 1. For a description of the units and reflecting surfaces, see Section 4.

lower than 10 cm. The data has been processed for tidal correction, removal of low-quality data points and generation of a data terrain model using the TELEDYNE PDS software.

4 | RESULTS

4.1 | Units and bounding surfaces

Three seismic units (Units 1–3) were found in the upper part of all of the studied seismic profiles, both in latitudinal and longitudinal directions (Figures 2 and 3, respectively). Each unit is bounded at its base by a channelised surface (S1–3). A relatively homogeneous seismic unit found below surface S1 is considered as the substrate (Unit S) of Units 1–3.

4.2 | Surface S1

Surface S1 separates Unit S (below) from Unit 1 (above) and corresponds to a relatively flat and gently seaward-inclined, high-amplitude reflector from *ca* 21 to 25 ms (TWT) (16.8–20 m) depth, considering a velocity of approximately 1600 m/s, a reasonable estimate for these

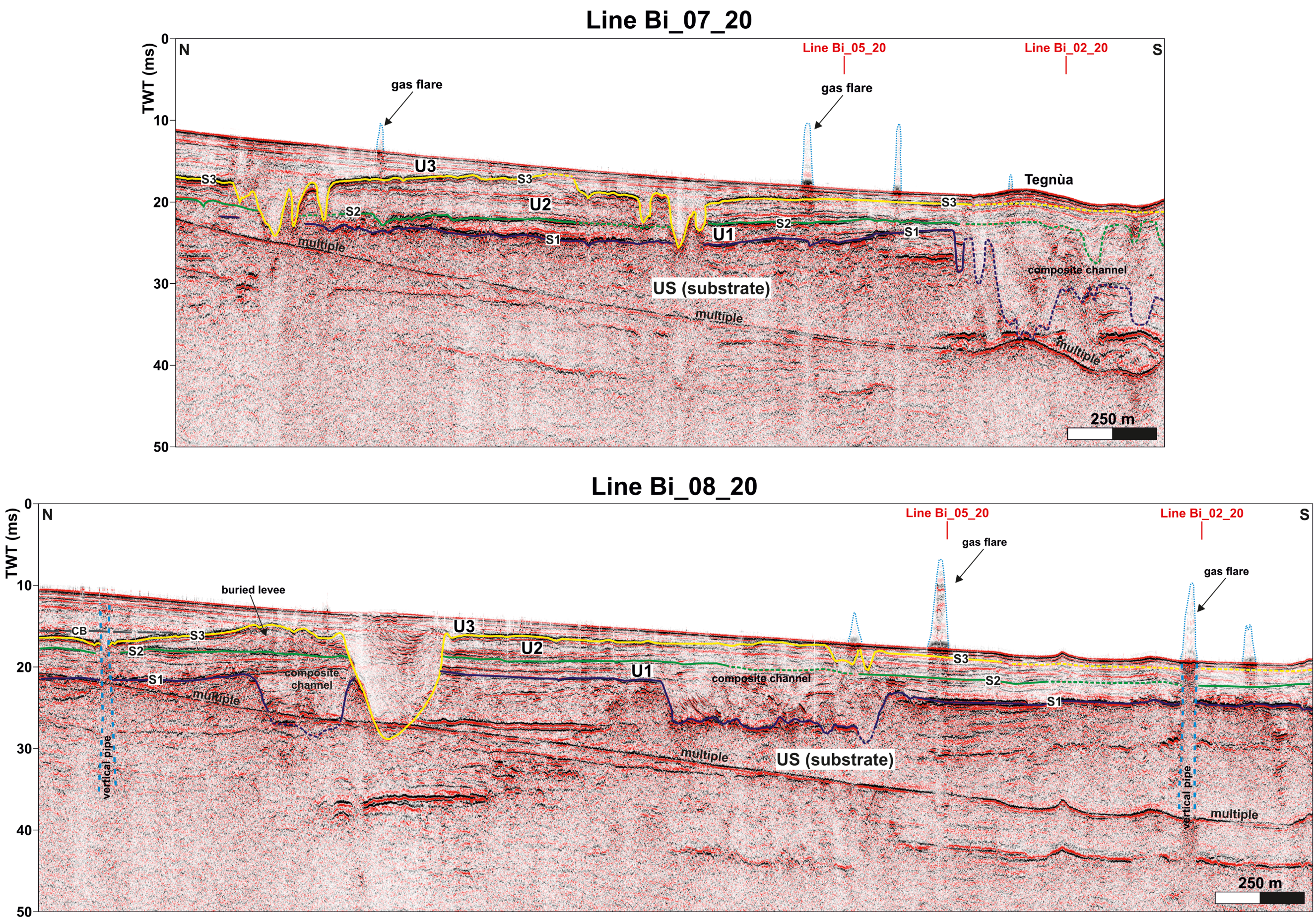

FIGURE 3 Interpreted seismic sections of the boomer data acquired in a longitudinal direction. The location of each line is indicated in Figure 1. For a description of the units and reflecting surfaces, see Section 4.

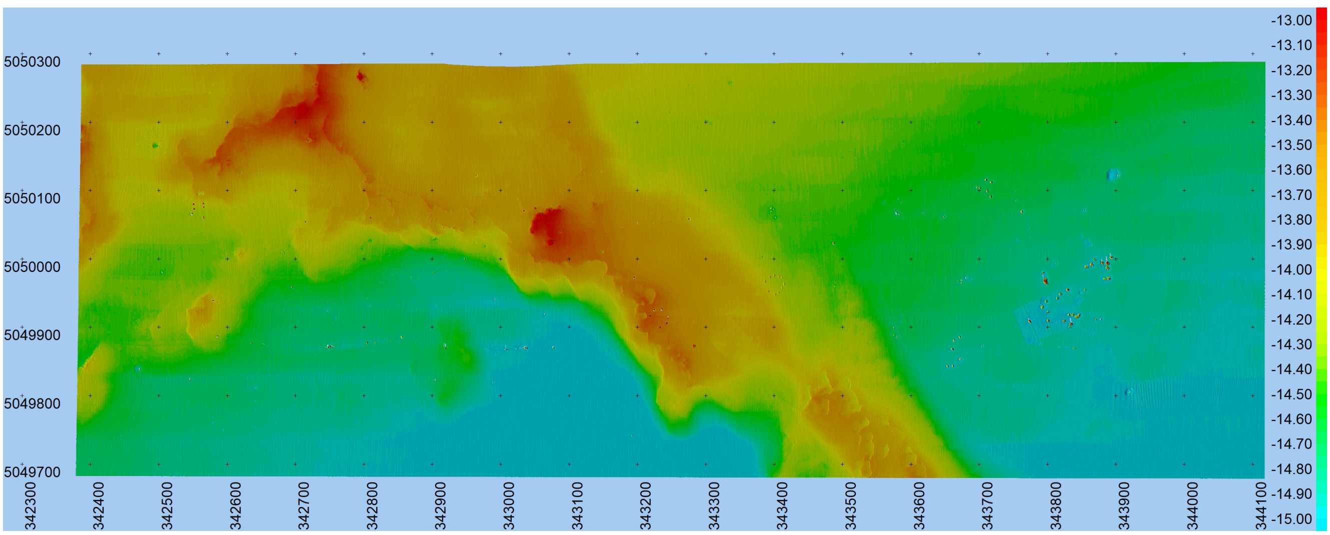

FIGURE 4 Results of the multibeam survey. See the dashed white rectangle in Figure 1 for the location of the multibeam survey.

shallow water-saturated sediments. Surface S1 is locally interrupted by composite V-shaped to U-shaped incisions up to 13 ms (TWT) (*ca* 10 m) deep (with respect to the adjacent flat surface) and over 500 m wide.

4.3 | Surface S2

Surface S2 separates Unit 1 (below) from Unit 2 (above) and coincides with a relatively flat to slightly irregular, medium-amplitude to high-amplitude reflector from *ca* 20 to 22 ms (TWT) (16–17.6 m) depth, interrupted by V-shaped incisions much less apparent than those associated with S1 (up to *ca* 3 m deep relative to the adjacent flat surface) and commonly developed in the same positions as in S1.

4.4 | Surface S3

Surface S3 separates Unit 2 (below) from Unit 3 (above) and coincides with a flat to irregular and gently seaward-inclined, medium-amplitude to high-amplitude reflector *ca* 17 to 21 ms (TWT) (13.6–16.8 m) depth, with associated isolated to composite V-shaped incisions up to *ca* 13 ms (TWT) (*ca* 10 m) deep (with respect to the adjacent flat surface) and up to 250 m wide. The deeper incisions may remove the underlying units, reaching Unit S. The relatively flat surfaces that separate the incisions locally show altimetric variations of *ca* 4 ms (TWT) (*ca* 3 m).

4.5 | Unit S

The features of Unit S are mainly recognisable in the upper part of the seismic profiles due to the masking effect of multiples. The unit is composed of sub-horizontal to gently inclined and undulated low-amplitude to high-amplitude reflectors showing local irregularities and minor incisions no more than 1 ms (TWT) deep. Higher amplitude sub-horizontal to irregular reflectors are locally evident; some segments of these reflectors can be classified as bright spots. The unit is crossed by several vertical pipes of variable width (from a few metres to 20–30 m), which blur or even whiten the signal.

4.6 | Unit 1

Unit 1, bounded by surfaces S1 and S2, ranges in thickness from less than 1 to *ca* 3 ms (TWT) in the flatter areas, but it is up to *ca* 15 ms (TWT) (up to 12 m) thick at the incisions on Unit S. Unit 1 is made up mostly of sub-horizontal to slightly undulate and gently inclined, low-amplitude to medium-amplitude reflectors, although the fillings of the incisions also contain irregularly inclined reflectors and a chaotic and locally transparent seismic facies. The vertical pipes crossing Unit S continue in Unit 1, masking the signal and locally producing a pull-up effect above surface S1.

4.7 | Unit 2

Unit 2, bounded by surfaces S2 and S3, ranges in thickness from *ca* 1 to 5 ms (TWT) (0.8–4 m) thick, and its changes in thickness mainly depend on the incisions associated with the bounding surfaces. The unit is composed of sub-horizontal to slightly undulate and gently inclined, low-amplitude to medium-amplitude reflectors. Convex-up reflectors locally form *ca* 500 m wide dome-like structures with an irregular top, bounded above by surface S3. This is most evident in Line Bi_08_20 (see Figure 3). The vertical pipes crossing Units S and 1 continue in Unit 2, masking the signal.

4.8 | Unit 3

Unit 3, bounded by surface S3 below and by the seabed above, ranges in thickness from *ca* 1 to 15 ms (TWT) (0.8–12 m), with the greater thicknesses at the incisions associated with S3. The unit exhibits a wedge shape in dip-oriented transects, where, not considering the filling of the incisions on S3, it markedly thins from proximal to distal locations. Relatively transparent, mainly concave-up reflectors characterise the incision fill, whereas gently seaward-inclined, low-amplitude to medium-amplitude reflectors downlapping surface S3 and the top of the fillings of the incisions characterise the wedge-shaped part of the unit. The distal part of the seismic profiles is characterised by dome structures on the seabed, *ca* 50 to 400 m wide and up to *ca* 3 ms (TWT) (2.4 m) high. The internal structure of these domes is not detectable due to the masking effect of seabed reflections. The vertical pipes crossing Units S, 1 and 2 continue in Unit 3 and above the sea floor, producing columnar gas flares up to 12 ms (TWT) (*ca* 10 m) high (see below).

4.9 | Gas-related features

The presence of shallow gas in all of the high-resolution seismic profiles (see Figures 2 and 3) is suggested by some gas-related features associated with signal anomalies: vertical gas pipes, associated with an upward migration of fluids and characterised by a poor-amplitude chaotic facies produced by the disruption of seismic reflectors with local pull-up effects; bright spots, indicating a fluid-charged sediment and characterised by high-amplitude and reverse polarity. Gas seeps from the sea floor are often associated with gas pipes. These seeps produce detectable amplitude anomalies known as flares.

5 | DISCUSSION

The features of Unit S resemble those of late Pleistocene continental deposits found below the Venice lagoon and in the adjacent marine area, mainly accumulated in alluvial plain to paludal environments (Zecchin et al., 2008, 2009, 2011, 2015). These settings are typically characterised by abundant gas seeps (vertical pipes) that are locally entrapped below more impermeable horizons consisting of peat beds and/or palaeosols (Zecchin et al., 2011), which appear as bright spots in seismic profiles.

Surfaces S1 and S2 probably correspond to surfaces of subaerial exposure, characterised by fluvial incisions (deeper in the case of surface S1) and adjacent interfluves that probably experienced paedogenesis (Posamentier & Allen, 1999; Zecchin et al., 2011). Units 1 and 2, therefore, are interpreted as fluvial deposits filling the incisions, passing laterally to floodplain deposits. The dome-like structures locally found in the upper part of Unit 2 are interpreted as aggrading channel-levee systems, a feature commonly observed in the late Pleistocene continental deposits of the northern Adriatic Sea (Zecchin et al., 2011; Tosi et al., 2017; Ronchi et al., 2023; Zecchin et al., 2024). Overall, the features of Units 1 and 2 are very similar to those of possibly coeval incised and infilled landforms found at similar depths below the sea floor in the northern Adriatic Sea, south-west of the study area by Ronchi et al. (2018), which were dated between *ca* 28 and 20 cal. ka BP.

The wedge shape of Unit 3, observed in dip-oriented transects, is very probably the result of relatively recent progradation of the coastal wedge during Holocene time (Zecchin et al., 2008, 2015; Tosi et al., 2017). The deep incisions characterising surface S3, therefore, could be the result of strong tidal flows producing tidal channels developed during the early Holocene transgressive phase (Ronchi et al., 2018) or tidal/inlet channels reworking older fluvial channels (Zecchin et al., 2009; Tosi et al., 2017). It is therefore inferred that the LGM surface developed at the top of Unit 2 and was later reworked by tidal currents and waves, producing tidal and wave-ravinement surfaces that sculpted the observed shape of surface S3. The S3 surface has also been identified along seismic lines acquired on land orthogonal to the shoreline (Accaino et al., 2023). The longitudinal lines Bi_07_20 and Bi_08_20 (Figure 3) are almost a continuation of such land lines, and continuity of the S3 surface from land to sea can therefore be inferred. Figure 5 shows an idealised evolutionary model of the studied succession from the pre-LGM (30 ka BP) to when the coastline reached the current position (*ca* 6 ka BP).

The considerable presence of gas in the analysed succession reflects what has been observed in the Plio-Quaternary sediments of the northern Adriatic Sea (Gordini et al., 2023). Analysis of the gas samples has shown that biogenic methane is the main component of gaseous emissions at the sea floor (Donda et al., 2019).

The presence of elongated mounds, up to 500 m long and 2.4 m high, can be clearly seen in the high-resolution seismic profiles (lines Bi-02-20 and Bi-07-20 in Figure 2) on the sea floor and in the morpho-bathymetry data, where they develop in a NW-SE direction (Figure 4). These morphological highs are interpreted as bio-concretioned

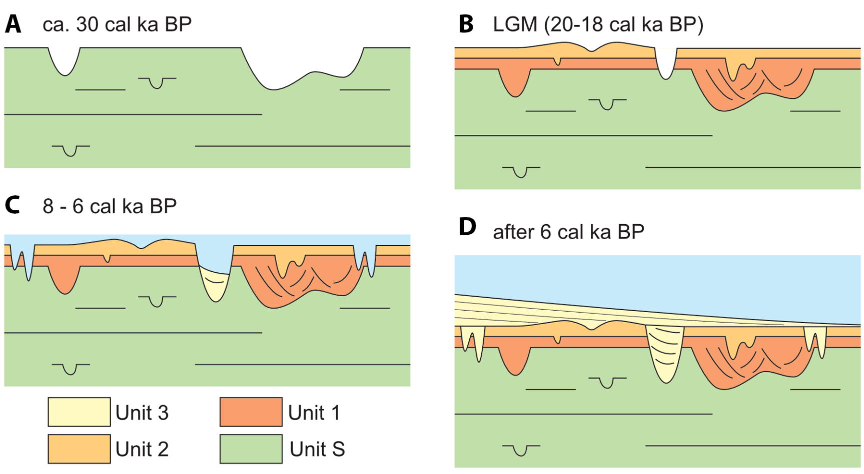

FIGURE 5 Evolutionary model of the studied succession shown with an idealised dip-oriented transect. (A) Subaerial exposure surface associated with river incision (surface S1) developed above alluvial plain sediments (Unit S) at *ca* 30 ka BP (see text). (B) After the accumulation of continental Unit 1 that filled older fluvial incisions, followed by the development of surface S2 and the accumulation of continental Unit 2, the LGM surface developed at the top of the latter. (C) The Holocene transgression led the formation of a shallow lagoon incised by tidal channels and inlets, which truncated all older units. (D) The Holocene highstand phase was characterised by the seaward progradation of the coastal wedge, which blanketed all previously accumulated deposits.

rocky build-ups grown on cemented sand bars, known as 'Tegnue' or 'Trezze' in the northern Adriatic Sea (Tosi et al., 2017). The 'Tegnue' are localised at a depth between 10 and 40 m and can exhibit up to 3 or 4 m of positive local relief above the surrounding sea floor. Typically, they are located 2–17 km from the coast and at depths between 8 and 22 m (Zecchin et al., 2015; Minelli et al., 2021; Gordini et al., 2023). The early lithification of sand, which represents the substrate of the build-ups, can be related either to the interaction between salt water and fresh submarine groundwater (Tosi et al., 2017) or to gas seeps (Donda et al., 2013, 2019; Gordini et al., 2023).

6 | CONCLUSIONS

The information provided by the surveys presented in this work is consistent with the known geology of the area, adding new information about the Quaternary sedimentary succession in an area of the northern Adriatic Sea that has not been the subject of prior investigation. Specifically, similar features to those found by Ronchi et al. (2018) were found, including deep incised valleys. Thanks to the analogies found with this work, which included laboratory analyses of core samples to date the sediments, an estimate of the age of the surfaces and units identified in the seismic lines has been supposed.

The presence of several gas chimneys seeping to the sea floor, as well as small formations including trapped gas ('bright spots'), is noted. Such gas, most probably of biogenic origin, can also reach the sea floor via gas chimneys, which are clearly visible on the seismic sections.

In order to investigate formations on the sea floor, boomer data were integrated with multibeam data. The domes found in both datasets appear to be of significant size, and their location and extension are consistent with those of the 'Tegnue', rocky outcrops typical of the Northern Adriatic.

As for the method here presented, the Boomer data appear to have excellent resolution and penetration capabilities for these shallow waters and sediment type, and its integration with the multibeam data are an excellent tool to detect the gas chimneys and the rocky outcrops ('Tegnue') on the sea floor.

ACKNOWLEDGEMENTS

This work was carried out within the ECOMAP Interreg Italy-Croatia project.

DATA AVAILABILITY STATEMENT

The data used in this paper can be provided upon request to the corresponding author.

ORCID

Federico Da Col https://orcid.org/0000-0002-1121-1001

REFERENCES

Accaino, F., Da Col, F., Böhm, G., Picotti, S., Giorgi, M., Meneghini, F. & Schleifer, A. (2023) Petro-physical characterization of the shallow sediments in a coastal area in NE Italy from the integration of active seismic and resistivity data. *Surveys in Geophysics*, 44, 1211–1238. https://doi.org/10.1007/s10712-023-09776-x

Amorosi, A., Dinelli, E., Rossi, V., Vaiani, S.C. & Sacchetto, M. (2008) Late Quaternary palaeoenvironmental evolution of the Adriatic coastal plain and the onset of Po River Delta. *Palaeogeography, Palaeoclimatology, Palaeoecology*, 268(1–2), 80–90. https://doi.org/10.1016/j.palaeo.2008.07.009

Anselmi, M., Govoni, A., De Gori, P. & Chiarabba, C. (2011) Seismicity and velocity structures along the south-Alpine thrust front of the Venetian Alps (NE-Italy). *Tectonophysics*, 513(1–4), 37–48. https://doi.org/10.1016/j.tecto.2011.09.023

Antonioli, F., Ferranti, L., Fontana, A., Amorosi, A., Bondesan, A., Braitenberg, C., Fontolan, G., Furlani, S., Mastronuzzi, G., Monaco, C., Spada, G. & Stocchi, P. (2009) Holocene relative sea-level changes and vertical movements along the Italian and Istrian coastlines. *Quaternary International.*, 206, 102–133. https://doi.org/10.1016/j.quaint.2008.11.008

Asioli, A., Trincardi, F., Lowe, J.J., Ariztegui, D., Langone, L. & Oldfield, F. (2001) Sub-millennial scale climatic oscillations in the central adriatic during the lateglacial: palaeoceanographic implications. *Quaternary Science Reviews*, 20, 1201–1221. https://doi.org/10.1016/S0277-3791(00)00147-5

Baradello, L. & Carcione, J.M. (2008) Optimal seismic-data acquisition in very shallow waters: surveys in the Venice lagoon. *Geophysics*, 73(6), Q59–Q63. https://doi.org/10.1190/1.2976117

Blum, M. & Törnqvist, T.E. (2000) Fluvial responses to climate and sea-level change: a review and look forward. *Sedimentology*, 47, 2–48. https://doi.org/10.1046/j.1365-3091.2000.00008.x

Blum, M., Martin, J., Milliken, K. & Garvin, M. (2013) Paleovalley systems: insights from Quaternary analogs and experiments. *Earth Science Reviews*, 116, 128–169. https://doi.org/10.1016/j.earscirev.2012.09.003

Bondesan, A. & Meneghel, M. (2004) *Geomorfologia della provincia di Venezia*. Padova: Esedra editrice.

Borga, M., Vezzani, C. & Fontana, G.D. (2005) Regional rainfall depth–duration–frequency equations for an alpine region. *Natural Hazards*, 36(1–2), 221–235. https://doi.org/10.1007/s11069-004-4550-y

Bortolami, G.C., Fontes, J.C., Markgraf, V. & Saliere, J.F. (1977) Land, sea and climate in the northern Adriatic region during Late Pleistocene. *Palaeogeography Palaeoclimatology Palaeoecology*, 21(2), 139–156. https://doi.org/10.1016/0031-0182(77)90010-4

Breda, A., Amorosi, A., Rossi, V. & Fusco, F. (2016) Late-glacial to Holocene depositional architecture of the Ombrone palaeovalley system (Southern Tuscany, Italy): sea-level, climate and local control in valley-fill variability. *Sedimentology*, 63, 1124–1148. https://doi.org/10.1111/sed.12253

Clement, A.J.H. & Fuller, I.C. (2018) Influence of system controls on the Late Quaternary geo-morphic evolution of a rapidly-infilled incised-valley system: the lower Manawatu valley, North Island New Zealand. *Geomorphology*, 303, 13–29.

Dallan, E., Borga, M., Zaramella, M. & Marra, F. (2022) Enhanced summer convection explains observed trends in extreme subdaily precipitation in the Eastern Italian Alps. *Geophysical Research Letters*, 49, e2021GL096727. https://doi.org/10.1029/2021GL096727

Donda, F., Civile, D., Forlin, E., Volpi, V., Zecchin, M., Gordini, E., Merson, E.B. & De Santis, L. (2013) The northernmost Adritaic Sea: a potential location for CO_2 geological storage? *Marine and Petroleum Geology*, 42, 148–159. https://doi.org/10.1016/j.marpetgeo.2012.10.006

Donda, F., Tinivella, U., Gordini, E., Panieri, G., Volpi, V., Civile, D., Forlin, E., Facchin, L., Burca, M., Cova, A. & Ferrante, G.M. (2019) The origin of gas seeps in the Northern Adriatic Sea. *Italian Journal Geosciences*, 138, 171–183. https://doi.org/10.3301/IJG.2018.34

Favero, V. & Serandrei Barbero, R. (1980) Origine ed evoluzione della laguna di Venezia–bacino meridionale. *Lavori della Societa' Veneziana di Scienze Naturali*, 5, 49–71.

Fontana, A. (2006) Evoluzione geomorfologica della bassa pianura friulana e sue relazione con le dinamiche insediative antiche. Enclosed Geological Map of the Low Friuli Plain Scale 47. Monografie Museo Friulano Storia Naturale, Udine, 288 pp.

Fontana, A., Mozzi, P. & Bondesan, A. (2008) Alluvial megafans in the Venetian-Friulian Plain (north-eastern Italy)_ Evidence of sedimentary and erosive phases during late Pleistocene and Holocene. *Quaternary International*, 189, 71–90. https://doi.org/10.1016/j.quaint.2007.08.044

Fontana, A., Bondesan, A., Meneghel, M., Toffoletto, F., Vitturi, A. & Bassan, V. (2010a) Note illustrative della Carta Geologica d'Italia alla scala 1:50.000. 107, Portogruaro. ISPRA-Regione del Veneto, Roma.

Fontana, A., Mozzi, P. & Bondesan, A. (2010b) Late pleistocene evolution of the Venetian–Friulian Plain. *Rendiconti Lincei*, 21(Suppl 1), S181–S196. https://doi.org/10.1007/s12210-010-0093-1

Fontolan, G., Pillon, S., Quadri, F.D. & Bezzi, A. (2007) Sediment storage at tidal inlets in northern Adriatic lagoons: ebb-tidal delta morphodynamics, conservation and sand use strategies. *Estuarine, Coastal and Shelf Science*, 75(1–2), 261–277. https://doi.org/10.1016/j.ecss.2007.02.029

Fontana, A. & Ronchi, L. (2019) Paesaggi sommersi in Alto Adriatico Dalla pianura glaciale al futuro innalzamento marino. *Studi e Ricerche*. https://doi.org/10.30687/978-88-6969-480-6/001

Francese, R., Bondesan, A. & Giorgi, M. (2014) Studio di zonazione geo-sismica della provincia di Venezia. RISVE Project, Provincia di Venezia.

Gatto, P. & Previatello, P. (1974) Significato stratigrafico, comportamento meccanico e distribuzione nella Laguna di Venezia di un'argilla sovraconsolidata nota come "Caranto". CNR. Laboratorio Studi Grandi Masse, T.R. 70, Venezia, 45 pp.

Ghielmi, M., Minervini, M., Nini, C., Rogledi, S., Rossi, M. & Vignolo, A. (2010) Sedimentary and tectonic evolution in the eastern Po-Plain and northern Adriatic Sea area from Messinian to Middle Pleistocene (Italy). *Rendiconti Lincei*, 21, 131–166. https://doi.org/10.1007/s12210-010-0101-5

Gordini, E., Donda, F., Tosi, L., Bergamasco, A., Bergamasco, A. & Donnici, S. (2023) The role of methane seepage in the formation of the Northern Adriatic Sea geosites. *Marine Geology*, 462, 107081. https://doi.org/10.1016/j.margeo.2023.107081

Minelli, A., Ferr'a, C., Spagnolo, A., Scanu, M., Tassetti, A.N., Ferrari, C.R., Mazziotti, C., Pigozzi, S., Jakl, S.Z., Sˇarcevi'c, T., Sˇimac, M., Kruschel, C., Pejdo, D., Barbone, E., De Gioia, M., Borme, D., Gordini, E., Auriemma, R., Benzon, I., Vukovi'c-Staniˇsi'c, D., Orli'c, S., Franci'c, V., Zec, D., Orli'c Kapovi'c, I., Soldati, M., Ulazzi, S. & Fabi, G. (2021) The ADRIREEF database: a comprehensive collection of natural/artificial reefs and wrecks in the Adriatic Sea. *Earth System Science Data*, 13, 1905–1923. https://doi.org/10.5194/essd-13-1905-2021

Ronchi, L., Fontana, A., Correggiari, A. & Asioli, A. (2018) Late Quaternary incised and infilled landforms in the shelf of the northern Adriatic Sea (Italy). *Marine Geology*, 405, 47–67. https://doi.org/10.1016/j.margeo.2018.08.004

Ronchi, L., Fontana, A., Cohen, K.M. & Stouthamer, E. (2021) Late Quaternary landscape evolution of the buried incised valley of Concordia Sagittaria (Tagliamento River, NE Italy): a reconstruction of incision and transgression. *Geomorphology*, 373, 107509. https://doi.org/10.1016/j.geomorph.2020.107509

Ronchi, L., Fontana, A., Novak, A., Correggiari, A. & Poglajen, S. (2023) Late-Quaternary evolution of the semi-confined alluvial megafan of Isonzo River (northern Adriatic): where the fluvial system of the southern Alps meets the Karst. *Geosciences*, 13, 135.

Slejko, D., Neri, G., Orozova, I., Renner, G. & Wyss, M. (1999) Stress field in Friuli (NE Italy) from fault plane solutions of activity following the 1976 main shock. *Bulletin of the Seismological Society of America*, 89, 1037–1052. https://doi.org/10.1785/BSSA0890041037

Pellegrini, C., Maselli, V., Gamberi, F., Asioli, A., Bohacs, K.M., Drexler, T.D. & Trincardi, F. (2017) How to make a 350-m-thick lowstand systems tract in 17,000 years: the Late Pleistocene Po River (Italy) lowstand wedge. *Geology*, 45, 327–330. https://doi.org/10.1130/G38848.1

Posamentier, H.W. & Allen, G.P. (1999) Siliciclastic sequence stratigraphy—concepts and applications. *SEPM Concepts in Sedimentology and Paleontology*, 7, 210.

Surian, N. & Fontana, A. (2017) The Tagliamento river: the fluvial landscape and long-term evolution of a large alpine braided river. In: Soldati, M. & Marchetti, M. (Eds.) *Landscapes and Landforms of Italy. World Geomorphological Landscapes*. Cham: Springer. https://doi.org/10.1007/978-3-319-26194-2_13

Thomas, M.A. & Anderson, J.B. (1989) Glacial eustatic controls on seismic sequences and parasequences of the Trinity/Sabine incised valley, Texas Continental Shelf. *Association of Geological Societies Transactions*, 39, 563–570.

Tosi, L., Zecchin, M., Franchi, F., Bergamasco, A., Da Lio, C., Baradello, L., Mazzoli, C., Montagna, P., Taviani, M., Tagliapietra, D., Carol, E., Franceschini, G., Giovanardi, O. & Donnici, S. (2017) Paleochannel and beach-bar palimpsest topography as initial substrate for coralligenous buildups offshore Venice, Italy. *Scientific Reports*, 7, 1321. https://doi.org/10.1038/s41598-017-01483-z

Zecchin, M., Baradello, L., Brancolini, G., Donda, F., Rizzetto, F. & Tosi, L. (2008) Sequence stratigraphy based on high-resolution seismic profiles in the late Pleistocene and Holocene deposits of the Venice area. *Marine Geology*, 253, 185–198. https://doi.org/10.1016/j.margeo.2008.05.010

Zecchin, M., Brancolini, G., Tosi, L., Rizzetto, F., Caffau, M. & Baradello, L. (2009) Anatomy of the Holocene succession of the southern Venice Lagoon revealed by very high-resolution seismic data. *Continental Shelf Research*, 29, 1343–1359. https://doi.org/10.1016/j.csr.2009.03.006

Zecchin, M., Caffau, M. & Tosi, L. (2011) Relationship between peat bed formation and climate changes during the last glacial in the Venice area. *Sedimentary Geology*, 238, 172–180. https://doi.org/10.1016/j.sedgeo.2011.04.011

Zecchin, M., Gordini, E. & Ramella, R. (2015) Recognition of a drowned delta in the northern Adriatic Sea, Italy: stratigraphic characteristics and its significance in the frame of the early Holocene sea-level rise. *The Holocene*, 25, 1027–1038. https://doi.org/10.1177/0959683615575358

Zecchin, M., Caffau, M., Busetti, M., Masoli, C.A., Baradello, L., Civile, D., Dal Cin, M., Petronio, L., Romeo, R., Zampa, L.S., Lenaz, D., Lucchi, R.G. & Caburlotto, A. (2024) Late Quaternary transgressions and regressions in the Trieste Gulf (north-eastern Adriatic Sea). *Quaternary International*. https://doi.org/10.1016/j.quaint.2024.03.001

How to cite this article: Da Col, F., Zecchin, M., Civile, D., Baradello, L., Deponte, M. & Accaino, F. (2024) Evolution of a late Quaternary succession by interpretation of high-resolution seismic and bathymetric data, Adriatic Sea. *The Depositional Record*, 00, 1–10. Available from: https://doi.org/10.1002/dep2.289